Current Biology 23, 2500–2505, December 16, 2013 ©2013 Elsevier Ltd All rights reserved http://dx.doi.org/10.1016/j.cub.2013.10.036

Report

Arabidopsis TOL Proteins Act as Gatekeepers for Vacuolar Sorting of PIN2 Plasma Membrane Protein

Barbara Korbei,[1,*] Jeanette Moulinier-Anzola,[1] Lucinda De-Araujo,[1] Doris Lucyshyn,[1] Katarzyna Retzer,[1] Muhammad A. Khan,[1,2] and Christian Luschnig[1,*]

[1]Department of Applied Genetics and Cell Biology, University of Natural Resources and Life Sciences, Vienna (BOKU), Muthgasse 18, 1190 Wien, Austria

Summary

Controlling variations in plasma membrane (PM) protein abundance is of utmost importance for development in higher plants. For modulating PM protein activity, endocytosed proteins can be either cycled between PM and endosomes or sorted for their irreversible inactivation to lysosomes/vacuoles. Cargo ubiquitination triggers vacuolar delivery for degradation, which is controlled by Endosomal Sorting Complex Required for Transport (ESCRT) [1, 2]. Essential parts of this machinery are conserved across kingdoms, but determinants liable for initial recognition and concentration of ubiquitinated cargo have not been identified in plants [3, 4]. Here, we describe members of an *Arabidopsis* TOL (*TO*M1-*L*IKE) family as ubiquitin binding proteins that act redundantly in control of plant morphogenesis. Specifically, *tol* mutant combinations exhibit defects that reflect alterations in responses mediated by the phytohormone auxin. Consistently, we provide evidence for a role of TOLs in recognition and further endocytic sorting of a PIN-FORMED (PIN)-type auxin carrier protein at the PM, modulating dynamic auxin distribution and associated growth responses. Such TOL-dependent vacuolar sorting depends on cargo ubiquitination and coincides with dynamic rearrangements in TOL distribution. Collectively, these findings lead us to suggest a function for TOLs early in the passage of endocytosed ubiquitinated PM cargo, acting as gatekeepers for degradative protein sorting to the vacuole.

Results and Discussion

In metazoa and fungi, ubiquitinated membrane protein cargos are captured by the heteromeric multivalent ubiquitin-binding complex ESCRT-0, until transferred to further ESCRT complexes for sorting toward the vacuole/lysosome [5]. In plants, characterized ESCRT counterparts do not localize principally to multivesicular bodies (MVB), as in metazoans, but are differentially distributed between *trans*-Golgi network/early endosome (TGN/EE) and MVBs [6]. Thus, loading of the ESCRT machinery occurs at earlier steps of endocytic sorting. Determinants responsible for initial recognition and concentration of ubiquitinated cargo, the ESCRT-0, have not been identified in plants [3].

Apart from ESCRT-0 subunits, TOM1 (target of myb) proteins, which are widely distributed in eukaryotes, contribute to loading of the ESCRT machinery and are postulated to function in parallel to or instead of the ESCRT-0 [7, 8]. Although orthologs of ESCRT-0 subunits are not found in higher plants [9], in silico analysis revealed an *Arabidopsis TOL* gene family with a modular domain structure similar to ESCRT-0 and TOM1 proteins, sharing an N-terminal VHS (Vps27, Hrs, and STAM) domain followed by a GAT (GGAs and TOM) domain and putative clathrin-binding motifs (Figures S1A and S1B available online). The VHS and GAT domains both mediate membrane association and ubiquitin binding [10–12]. *At*TOL proteins combine all functionally relevant domains, sufficient for recognition and sorting of ubiquitinated cargo.

All nine predicted *TOL* loci are expressed in wild-type; thus, none is likely to represent a pseudogene (Figure S2A). We identified T-DNA insertion mutants for all loci, which fail to express full-length *TOL* transcripts, presumably representing loss-of-function alleles (Figure 2A). Homozygous single mutants are viable and show no obvious phenotype. When generating all double-mutant combinations (Figure S2B), two combinations (*tol5-1/tol8-1* and *tol7-1/tol8-1*) could not be obtained as homozygotes (>100 F2 individuals analyzed). Examination of siliques on F1 plants, heterozygous for one of these particular *tol* mutants, indicated aborted seed development in a mendelian 3:1 ratio (alive:aborted = 203:75; X^2 = 0.580, p = 0.4462; Figure S2B), a segregation consistent with early embryogenesis defects of homozygous double mutants. All other *tol* double mutants do not exhibit apparent phenotypes, indicative of functional redundancy within the gene family.

Higher-order mutant combinations have been generated, and the *tol2-1/tol3-1/tol5-1/tol6-1/tol9-1* quintuple mutant (*tolQ*) produced an array of pronounced morphogenetic defects (Figure 1). Similar, but less severe defects were observed in *tol2-1/tol3-1/tol6-1/tol9-1* and *tol3-1/tol5-1/tol6-1/tol9-1*, whereas triple mutants and further quadruple combinations were without apparent mutant phenotype.

tolQ seedlings are delayed in their development and exhibit reduced germination frequency (germination $\geq$80%; n = 435). A large fraction of *tolQ* seedlings displays altered cotyledon formation ($\geq$70%; n = 240; monocots, tricots, or fused cotyledons) highlighting aberrations during embryogenesis (Figure 1A). Aerial portions of mature plants are dwarfed and delayed in flowering (Figure 1C) and show anomalous inflorescence and floral morphology, discernible by fused floral organs with two or three pistils and ectopic positioning of siliques (Figure 1B). Nevertheless, *tolQ* is fertile, although it exhibits reduced fecundity.

tolQ has defects in root meristem morphology, reflected in a smaller meristematic zone (Figure S2C) and variations in the organization of stem cell niche and columella root cap (Figure 1D). *tolQ* forms shorter primary roots (*TOL* = 118 ± 14 mm; *tolQ* = 75 ± 35 mm at 14 DAG; n = 60) and develops less lateral roots (Figure 1E). Furthermore, we observed a significant delay in the reorientation of root growth in response to gravity (Figure 1F), all representing aspects of morphogenesis that are influenced by the phytohormone auxin. To further

[2]Present address: Department of Bioinformatics and Biotechnology, Government College University, Faisalabad 38000, Pakistan

*Correspondence: barbara.korbei@boku.ac.at (B.K.), christian.luschnig@boku.ac.at (C.L.)

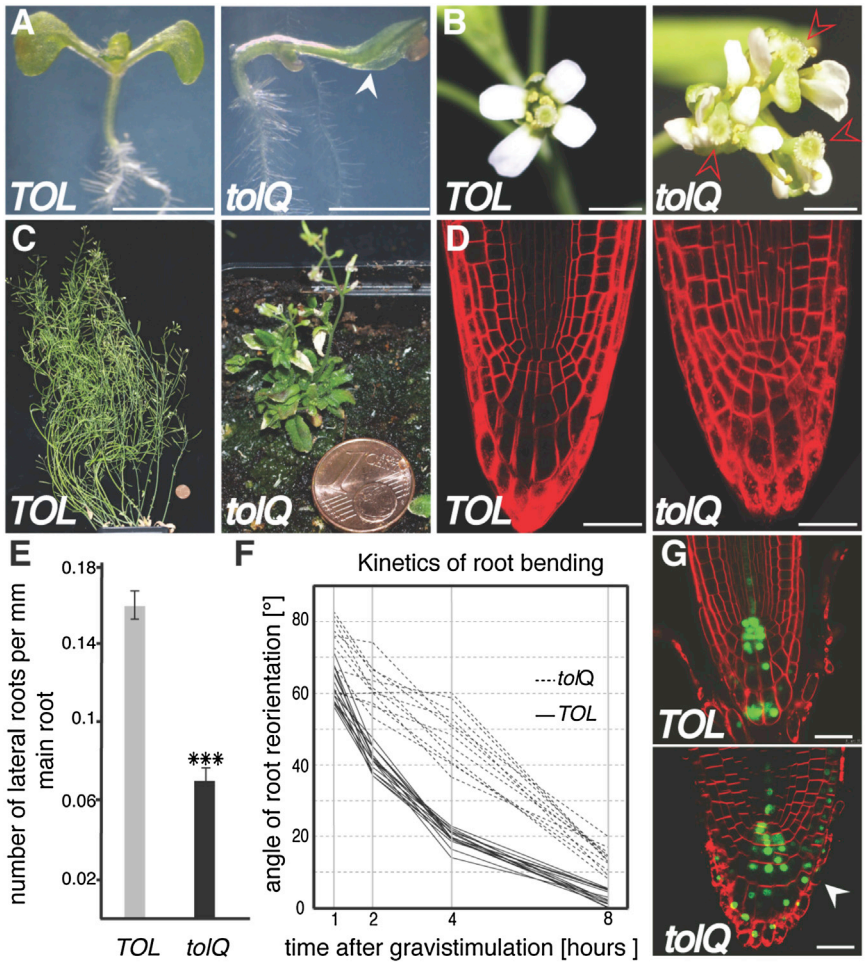

Figure 1. Phenotypic Analysis of *tolQ*

(A) Wild-type *TOL* and *tolQ* seedlings, 7 days after germination (DAG); arrowhead, single cotyledon.

(B) *TOL* and *tolQ* inflorescences; arrowheads, multiple ectopic pistils.

(C) Adult *TOL* and *tolQ* plant, 10-week-old.

(D) Root meristem morphology in *TOL* and *tolQ* seedlings 7 DAG, stained with FM4-64.

(E) Number of lateral roots per mm of primary root in 2-week-old *TOL* and *tolQ* seedlings (n = 3, 60 roots analyzed, mean ± SD, ***$p \leq 0.001$).

(F) Reorientation of root growth after gravistimulation for indicated time intervals (n = 3, 15 roots analyzed).

(G) Expression of *DR5rev::3XVENUS-N7* (green) in *TOL* and *tolQ* root tips counterstained with FM4-64 (red) 7 DAG. Arrowhead, VENUS signals in lateral portions. Eighty-six percent of the *tolQ* roots (n = 37) showed this effect, not detectable in *TOL* roots (n = 28) using same CLSM settings.

Scale bars represent 5 mm in (A); 2 mm in (B); and 25 μm in (D) and (G). See also Figure S2.

determine auxin responses, we viewed expression of auxin-responsive *pDR5rev::3xVENUS-N7* [13]. Control seedlings showed VENUS expression in quiescent center and root cap columella cells, whereas in *tolQ*, signals extended further into lateral portions of the root meristem, indicative of deviations in auxin distribution or signaling (Figure 1G). Taken together, pleiotropic defects of *tolQ* indicate essential roles for *TOL* genes in plant development, with deficiencies in auxin-controlled growth events underlining a function in plant hormonal signaling.

Because TOM1 and ESCRT-0 proteins mediate recognition of ubiquitinated plasma membrane (PM) protein via interaction with ubiquitin [8, 14] and required domains are conserved in TOLs, we tested for their ubiquitin binding by in vitro pull-down assays. GST-ubiquitin fusion and GST-tag alone, immobilized on gluthathione beads, were used to precipitate bacterially expressed, purified His-tagged TOLs. As a control, we employed GST:ubq^{I44A}, in which ubiquitin isoleucin 44, critical for recognition by ubiquitin binding

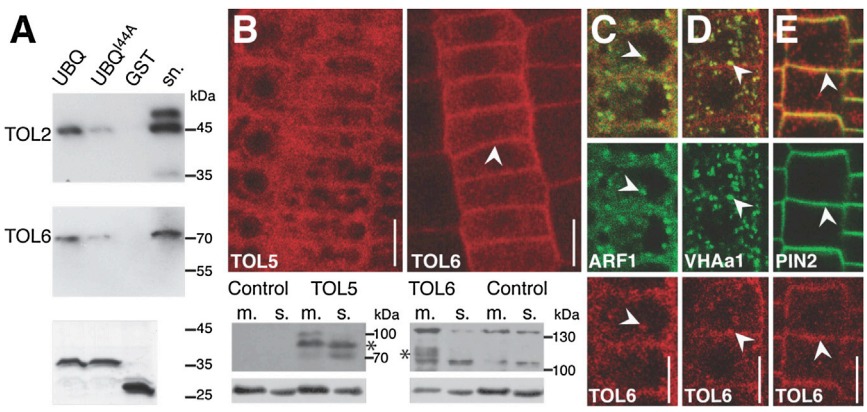

Figure 2. Ubiquitin-Binding Activity and Localization of TOL Proteins

(A) TOL2:6xHis (43 kDa) and TOL6:6xHis (75 kDa) coprecipitated with GST:ubq (34.5 kDa), GST:ubq^{I44A} (34.5 kDa), or GST (26 kDa), coupled to glutathione Sepharose. Precipitates probed with anti-His antibody (top two panels). Coomassie staining of proteins bound to beads demonstrates comparable amounts of protein used (bottom panel).

(B) Top: signal distribution of *TOL5p::TOL5:mCherry* in *tol5-1* and *TOL6p::TOL6:mCherry* in *tol6-1* root meristem cells (6 DAG). Arrowhead, signal in proximity to transversal cell walls. Bottom: membrane (m.) and soluble (s.) protein extracts from *tol5-1 TOL5p::TOL5:mCherry*, *tol6-1 TOL6p::TOL6:mCherry* and Col-0 probed with anti-mCherry. Asterisks, position of TOL5:mCherry and TOL6:mCherry. Tubulin (α-TUB) was used to visualize protein loading.

(C–E) *TOL6p::TOL6:mCherry* (red) coexpressed with TGN/EE marker *ARF1p::ARF1:GFP* (C; green), *VHAa1p::VHAa1:GFP* (D; green), and with PM marker *PIN2p::PIN2:GFP* (E; green). Images show *tol6-1* root meristem epidermis cells at 6 DAG. Arrowheads, colocalization of reporter signals.

Scale bars represent 10 μm. See also Figure S3.

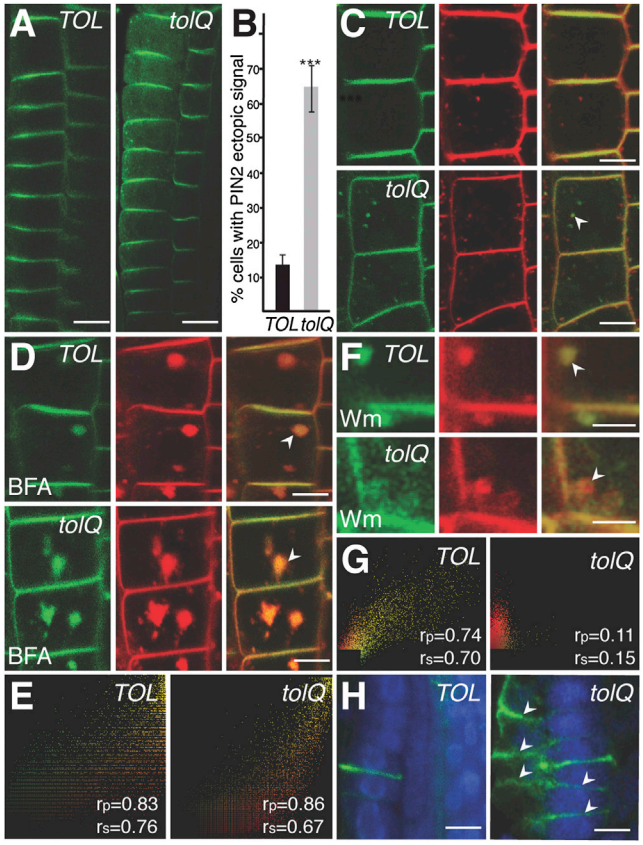

Figure 3. Endosomal Sorting in *tolQ*

(A) Confocal images of anti-PIN2 immunolocalization in *TOL* and *tolQ* seedlings 5 DAG.

(B) Percentage of epidermal cells with intracellular PIN2 aggregates in 5 DAG *TOL* and *tolQ* seedlings (n = 3, 30 roots analyzed, ten epidermal cells analyzed per root, mean ± SD, ***$p \leq 0.001$).

(C) PIN2:VENUS (green) localization in *TOL* and *tolQ* root meristem cells. Intracellular PIN2:VENUS in *tolQ* partially colocalizes with EE that stain after 15 min incubation with FM4-64 (red; arrowhead).

(D) PIN2:VENUS (green) in *TOL* and *tolQ* root meristem cells cotreated with BFA (25 μM), CHX (50 μM), and FM4-64 (red) for 90 min. Accumulation of PIN2:VENUS in BFA compartments (arrowheads).

(E) Pearson (r_p) and Spearman (r_s) correlation coefficients of PIN2:VENUS and FM4-64 signal colocalization in BFA compartments. High correlation coefficients: good colocalization.

(F) Root meristem cells of *TOL* and *tolQ PIN2p::PIN2:VENUS* seedlings treated with Wm (33 μM) and CHX (50 μM) for 90 min, counterstained with FM4-64 (red). In *TOL*, PIN2:VENUS accumulates in Wm compartments (arrowhead), whereas only limited colocalization is observed in *tolQ* (arrowhead).

(G) r_p and r_s correlation coefficients of PIN2:VENUS and FM4-64 signal colocalization in Wm compartment are markedly reduced in *tolQ*.

(H) Confocal images of KNOLLE (green) immunolocalization in *TOL* and *tolQ* seedlings 5 DAG, costained with DAPI to visualize nuclei (blue). Arrowheads, ectopic KNOLLE signals in proximity of transversal cell boundaries. Scale bars represent 10 μm in (A) and (H); 5 μm in (C) and (D); and 2 μm in (F). See also Figure S4.

domains (UBDs) like GAT and VHS domains, has been replaced by alanine [12]. These assays revealed that GST:ubq can pull down TOL2:6xHis and TOL6:6xHis, whereas binding was substantially reduced with GST:ubq^{I44A}, and no specific interaction was observed when using GST (Figure 2A). This provides evidence for the functionality of predicted TOL UBDs, which appear to exhibit binding specificities similar to nonplant VHS/GAT domain [12].

To investigate *TOL* expression, reporter constructs of *TOL5* and *TOL6*, as *TOL* representatives, whose loss contributes to defects in *tolQ*, were generated. GUS staining of promoter-reporter lines gave ubiquitous staining throughout *TOL5p::GUS* seedlings (Figure S3A). Furthermore, confocal laser scanning microscopy analysis (CLSM) of functional *TOL5p::TOL5:mCherry* and *TOL6p::TOL6:mCherry* reporters (Figure S3B) revealed punctate intracellular signals, together with pronounced signal at the cellular periphery and the cell plate of dividing cells (Figures 2B and S3C). When probing protein distribution in cellular fractions, we detected TOL5:mCherry in soluble and membrane fractions, whereas TOL6:mCherry accumulated preferentially in the pellet fraction, indicative of membrane association (Figure 2B, bottom panels).

TOL6:mCherry, partially colocalized with TGN/EE markers ARF1:GFP and VHAa1:GFP, but not with late endosomal marker ARA7:GFP and tonoplast marker Wave9Y (Figures 2C, 2D, and S3D). TOL6 localization close to or at the PM is underlined by a marked overlap with signals of PIN2:GFP, an intrinsic PM protein (Figure 2E). However, unlike PM proteins, which accumulate in recycling endosomal compartments upon treatment with sorting inhibitor brefeldin A (BFA) [15], or wortmannin (Wm), which inhibits formation of intraluminal vesicles of MVBs [16], distribution of TOL6:mCherry signals is not visibly affected by these drugs (Figure S3E).

Taken together, TOL-mCherry localization at early endosomal structures and proximal to the PM is consistent with a function in early steps of cargo recognition or sorting.

To characterize the role of TOLs in PM cargo sorting, we analyzed localization of membrane proteins [17, 18]. PIN2 auxin carrier exhibits polar distribution at the PM of lateral root cap, epidermis, and cortical root meristem cell files, controlling polar auxin transport into the elongation zone [19]. PIN2 ubiquitination acts as a signal for its internalization from the PM and further sorting into the lytic vacuole; thus, the protein represents a potential substrate for TOLs [17]. PIN2 immunostaining of *tolQ* primary root meristems revealed polar signal distribution similar to Col-0 controls, suggesting that PIN2 polar sorting is not significantly affected by TOLs (Figure 3A). However, we observed ectopic PIN2 signals in punctate structures, also detectable when viewing *PIN2::PIN2:VENUS* in *tolQ* (Figures 3A–3C). Ectopic PIN2:VENUS signals partially colocalized with EE (Figure 3C), indicated by signal overlaps with the endocytosed styryl dye FM4-64, but not with vacuoles (Figure S4A). Ectopic PIN2 accumulation is not the result of general defects in endocytosis toward vacuolar compartments, because we observed comparable sorting kinetics of endocytosed FM4-64 and vacuolar morphologies in *TOL* and *tolQ* (Figure S4B).

To dissect PIN2:VENUS sorting in *tolQ*, we performed treatments with trafficking inhibitors. First, we treated seedlings with cycloheximide (CHX; translational inhibitor) and BFA, to block PIN2 trafficking between endosomes and PM, causing protein accumulation in intracellular BFA compartments [15]. No significant differences in intracellular PIN2:VENUS accumulation were detected in *TOL* and *tolQ* (Figures 3D, 3E, and S4C), suggesting that PIN2 sorting into BFA compartments is not affected by TOLs. When treating with Wm, control seedlings responded with formation of enlarged MVBs that colocalized with PIN2 reporter, as demonstrated previously [20] (Figures 3F and S4C). In *tolQ*, however, we observed only limited colocalization between PIN2:VENUS signals and Wm

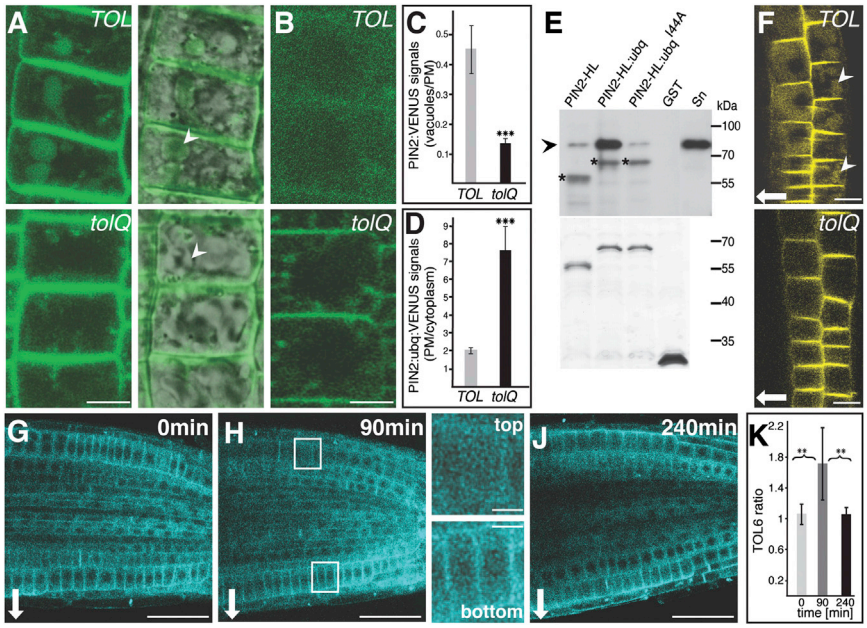

Figure 4. TOL Proteins and Sorting of PIN2

(A) PIN2:VENUS (green) in *TOL* and *tolQ* root meristems 6 DAG, after 5 hr of dark incubation (arrowheads, vacuoles).

(B) PIN2:ubq:VENUS in *TOL* and *tolQ* root epidermis cells 6 DAG.

(C) Relative signal intensities of PIN2:VENUS in *TOL* and *tolQ* vacuoles after dark incubation normalized to signals at the PM.

(D) Relative PIN2:ubq:VENUS signal intensities at the PM of *TOL* and *tolQ* root meristem cells normalized to cytoplasmic signal intensities (n = 3, 18 seedlings analyzed for each genotype, eight cells analyzed for each seedling, in (C) and (D), mean ± SD; ***$p \leq 0.001$).

(E) TOL6:6xHis coprecipitated with GST:PIN2-HL, GST:PIN2-HL:ubq, GST:PIN2-HL:ubq^{I44A}, or GST; probed with anti-His antibody (top; arrowhead, TOL6:6xHis; asterisk, GST-PIN2-HL; Sn, supernatant). Coomassie staining demonstrates similar amounts of GST-tagged proteins used (bottom).

(F) PIN2:VENUS (yellow) in *TOL* and *tolQ* root meristems gravistimulated for 90 min. Arrowheads, reporter signals in vacuoles at the upper side of *TOL* roots (*TOL* = 7, n = 15; *tolQ* = 0, n = 12).

(G–J) TOL6:mCherry (blue) in gravistimulated roots after 0 (G), 90 (H), and 240 (J) min of stimulation (white squares, areas displayed to the right).

(K) Relative TOL6:mCherry signal intensities proximal to transverse cell walls of root epidermis cells at the lower versus the upper side of gravistimulated roots (n = 3, 15 seedlings for each time point, ten cells analyzed from upper and lower epidermis for each seedling, mean ± SD; **$p \leq 0.01$, brackets indicate data sets compared by t test).

Scale bars represent 5 μm in (A), (B), and (H); 10 μm in (F); and 50 μm in (G), (H), and (J); arrows show the direction of the gravity vector.

compartments, emphasizing trafficking defects in the passage to the vacuole (Figures 3F, 3G, and S4C).

When testing localization of further PM localized proteins such as PIN1 and PM-H$^+$-ATPase in root meristem cells, we observed no apparent differences in *tolQ*, suggesting that sorting of these proteins is not significantly altered at this developmental stage (Figures S4D and S4E). Divergently, the syntaxin KNOLLE (KN), which is normally found at the cell plate of dividing cells, and is subsequently sorted to the lytic vacuole [21], accumulated ectopically in the periphery of *tolQ* root cells not actively proceeding though cytokinesis, (Figure 3H). This could reflect deficiencies in efficient removal of KN after cytokinesis has been completed, further supporting a function for TOLs in vacuolar sorting events.

We further analyzed PIN2:VENUS vacuolar accumulation in seedlings, dark incubated to promote stabilization of fluorescent protein-tagged reporters in the lytic compartment [22]. Whereas controls exhibited strong vacuolar accumulation, the signal was more than 3-fold reduced in *tolQ*, reflecting diminished vacuolar PIN2 (Figures 4A and 4C). Next, we analyzed a PIN2-ubiquitin fusion protein, constitutively targeted to the lytic vacuole due to its ubiquitin moiety [17, 23]. This effect is blocked upon mutagenesis of ubiquitin isoleucin 44, essential for interaction with UBDs [12], indicating that destabilization of PIN2-ubiquitin depends on recognition by ubiquitin-binding proteins [17]. Expression of *PIN2p::PIN2:ubq:VENUS* in *tolQ* resulted in VENUS signals at the PM almost 4-fold stronger than in *PIN2p::PIN2:ubq:VENUS* controls (Figures 4B and 4D), demonstrating that TOLs are required for vacuolar targeting of constitutively ubiquitinated PIN2. Moreover, a preferential signal of PIN2:ubq:VENUS at the PM in *tolQ* implies TOL participation in early endocytic sorting events, similar to mammalian TOM1L1 [24].

We tested TOL binding to PIN2-ubiquitin in assays, performed with different versions of the central hydrophilic PIN2 loop region (PIN2-HL) fused to GST. These binding studies revealed GST:PIN2-HL:ubq interaction with His-tagged TOL6, whereas no specific interaction was observed when using mutated GST:PIN2-HL:ubq^{I44A}, GST:PIN2-HL or GST (Figure 4E). Thus, TOL interaction requires recognition of the ubiquitin moiety expressed in frame with PIN2, supporting a scenario in which TOL proteins modulate intracellular sorting of ubiquitinated PIN2.

PIN2 vacuolar targeting has been linked to root gravitropism, mediating root growth along the gravity vector [25, 26]. At the upper epidermis of horizontally positioned root tips, vacuolar targeting of PIN2 reinforces establishment of lateral auxin gradients, causing downward bending of the root [25]. We analyzed vacuolar accumulation of *PIN2:VENUS* in the upper epidermis of gravistimulated *tolQ* and observed markedly less vacuolar signal than in the controls (Figure 4F), linking TOL function to differential PIN2 sorting in gravity-responding roots.

Next, we analyzed TOL6 distribution in gravistimulated roots. Immediately after stimulation, TOL6:mCherry exhibits equal signal distribution in upper and lower epidermis cells of horizontally positioned roots (Figure 4G). After 90 min, however, a gradient is clearly discernible, with approximately twice as much TOL6:mCherry (Figures 4H and 4K) in proximity of PM domains at the lower side than at the upper side, where signal are comparably diffuse. After prolonged incubation, this asymmetry is reversed and TOL6 is once more localized symmetrically in the root meristems (Figures 4J and 4K). These variations in TOL6:mCherry distribution are reminiscent of variable PIN2 distribution upon gravistimulation [25] and point to dynamic adjustments in TOL-controlled endocytic sorting processes.

Our experiments indicate that TOLs function in recognition of ubiquitinated cargo at PM domains, initiating a cascade of events that guide cargo to the vacuole. This activity appears

relevant to sorting of developmental determinants, whose expression involves rapid and tight control of protein abundance, whereas comparably stable proteins might be less affected. Consistent with this, we found variations in TOL6 distribution mirroring their role in PIN2 degradation during gravistimulation. This might involve either participation in early steps of cargo endocytosis, as indicated by internal TOL6 signals in cell files at the upper side of roots, or TOL accumulation at the PM of lower epidermis cells, promoting resetting of PIN2 levels during later stages of gravitropic root growth to avoid excess root bending [27]. Thus, spatiotemporal variations in TOL-mediated cargo recognition and sorting contribute to establishment PIN2 gradients in gravistimulated roots. This offers a plausible explanation for delay in gravitropic root bending response in *tolQ* and underlines critical roles for TOLs in fine-tuning auxin distribution. Although we focused on PIN2, pleiotropic *tolQ* growth defects and localization studies indicate TOL involvement in recognition of additional substrates such as KN.

Among multicellular organisms, higher plants represent the only phylogenetic branch that does not encode ESCRT-0 subunits, although a role for ESCRT in vacuolar delivery of ubiquitinated proteins has been demonstrated [28]. Instead, plant genomes are characterized by extended families of TOM-like proteins [3], necessary and sufficient to compensate for the absence of ESCRT-0 [7]. Our findings suggest that life without ESCRT-0 could be accounted for by TOL proteins, functioning as principal gating factors for recognition of ubiquitinated cargo. Detailed insights into mechanisms of TOL-cargo interaction as well as crosstalk with established components of the endocytic sorting machinery, however, will be subject to future studies.

Supplemental Information

Supplemental Information includes Supplemental Experimental Procedures, four figures, and one table and can be found with this article online at http://dx.doi.org/10.1016/j.cub.2013.10.036.

Acknowledgments

We are indebted to B. Scheres, J. Kleine-Vehn, K. Schumacher, N. Geldner, T. Gaude, G. Jürgens, J. Friml, and M. Heisler for providing published material. We thank J. Kleine-Vehn and C. Löfke for valuable comments and discussion and L. Abas and M.T. Hauser for their support and interest. L.D.-A. was supported by the Ministry of Science and Technology (Mozambique), K.R. by the ÖAW, and M.A.K. by the HEC. This work was supported by a Hertha Firnberg fellowship and by the Austrian Science Fund (FWF; B.K., T477; C.L., P19585, P25931).

Received: July 10, 2013
Revised: September 20, 2013
Accepted: October 15, 2013
Published: December 5, 2013

References

1. Williams, R.L., and Urbé, S. (2007). The emerging shape of the ESCRT machinery. Nat. Rev. Mol. Cell Biol. *8*, 355–368.
2. Raiborg, C., and Stenmark, H. (2009). The ESCRT machinery in endosomal sorting of ubiquitylated membrane proteins. Nature *458*, 445–452.
3. Winter, V., and Hauser, M.T. (2006). Exploring the ESCRTing machinery in eukaryotes. Trends Plant Sci. *11*, 115–123.
4. Shahriari, M., Richter, K., Keshavaiah, C., Sabovljevic, A., Huelskamp, M., and Schellmann, S. (2011). The Arabidopsis ESCRT protein-protein interaction network. Plant Mol. Biol. *76*, 85–96.
5. Hurley, J.H. (2010). The ESCRT complexes. Crit. Rev. Biochem. Mol. Biol. *45*, 463–487.
6. Scheuring, D., Viotti, C., Krüger, F., Künzl, F., Sturm, S., Bubeck, J., Hillmer, S., Frigerio, L., Robinson, D.G., Pimpl, P., and Schumacher, K. (2011). Multivesicular bodies mature from the trans-Golgi network/early endosome in Arabidopsis. Plant Cell *23*, 3463–3481.
7. Herman, E.K., Walker, G., van der Giezen, M., and Dacks, J.B. (2011). Multivesicular bodies in the enigmatic amoeboflagellate Breviata anathema and the evolution of ESCRT 0. J. Cell Sci. *124*, 613–621.
8. Shields, S.B., and Piper, R.C. (2011). How ubiquitin functions with ESCRTs. Traffic *12*, 1306–1317.
9. Schellmann, S., and Pimpl, P. (2009). Coats of endosomal protein sorting: retromer and ESCRT. Curr. Opin. Plant Biol. *12*, 670–676.
10. Ren, X., and Hurley, J.H. (2010). VHS domains of ESCRT-0 cooperate in high-avidity binding to polyubiquitinated cargo. EMBO J. *29*, 1045–1054.
11. Prag, G., Watson, H., Kim, Y.C., Beach, B.M., Ghirlando, R., Hummer, G., Bonifacino, J.S., and Hurley, J.H. (2007). The Vps27/Hse1 complex is a GAT domain-based scaffold for ubiquitin-dependent sorting. Dev. Cell *12*, 973–986.
12. Dikic, I., Wakatsuki, S., and Walters, K.J. (2009). Ubiquitin-binding domains - from structures to functions. Nat. Rev. Mol. Cell Biol. *10*, 659–671.
13. Heisler, M.G., Ohno, C., Das, P., Sieber, P., Reddy, G.V., Long, J.A., and Meyerowitz, E.M. (2005). Patterns of auxin transport and gene expression during primordium development revealed by live imaging of the Arabidopsis inflorescence meristem. Curr. Biol. *15*, 1899–1911.
14. Wang, T., Liu, N.S., Seet, L.F., and Hong, W. (2010). The emerging role of VHS domain-containing Tom1, Tom1L1 and Tom1L2 in membrane trafficking. Traffic *11*, 1119–1128.
15. Geldner, N., Anders, N., Wolters, H., Keicher, J., Kornberger, W., Muller, P., Delbarre, A., Ueda, T., Nakano, A., and Jürgens, G. (2003). The Arabidopsis GNOM ARF-GEF mediates endosomal recycling, auxin transport, and auxin-dependent plant growth. Cell *112*, 219–230.
16. Robinson, D.G., Jiang, L., and Schumacher, K. (2008). The endosomal system of plants: charting new and familiar territories. Plant Physiol. *147*, 1482–1492.
17. Leitner, J., Petrášek, J., Tomanov, K., Retzer, K., Pařezová, M., Korbei, B., Bachmair, A., Zažímalová, E., and Luschnig, C. (2012). Lysine63-linked ubiquitylation of PIN2 auxin carrier protein governs hormonally controlled adaptation of Arabidopsis root growth. Proc. Natl. Acad. Sci. USA *109*, 8322–8327.
18. Spitzer, C., Reyes, F.C., Buono, R., Sliwinski, M.K., Haas, T.J., and Otegui, M.S. (2009). The ESCRT-related CHMP1A and B proteins mediate multivesicular body sorting of auxin carriers in Arabidopsis and are required for plant development. Plant Cell *21*, 749–766.
19. Blilou, I., Xu, J., Wildwater, M., Willemsen, V., Paponov, I., Friml, J., Heidstra, R., Aida, M., Palme, K., and Scheres, B. (2005). The PIN auxin efflux facilitator network controls growth and patterning in Arabidopsis roots. Nature *433*, 39–44.
20. Jaillais, Y., Fobis-Loisy, I., Miège, C., Rollin, C., and Gaude, T. (2006). AtSNX1 defines an endosome for auxin-carrier trafficking in Arabidopsis. Nature *443*, 106–109.
21. Reichardt, I., Stierhof, Y.D., Mayer, U., Richter, S., Schwarz, H., Schumacher, K., and Jürgens, G. (2007). Plant cytokinesis requires de novo secretory trafficking but not endocytosis. Curr. Biol. *17*, 2047–2053.
22. Laxmi, A., Pan, J., Morsy, M., and Chen, R. (2008). Light plays an essential role in intracellular distribution of auxin efflux carrier PIN2 in Arabidopsis thaliana. PloS One *3*, e1510.
23. Herberth, S., Shahriari, M., Bruderek, M., Hessner, F., Müller, B., Hülskamp, M., and Schellmann, S. (2012). Artificial ubiquitylation is sufficient for sorting of a plasma membrane ATPase to the vacuolar lumen of Arabidopsis cells. Planta *236*, 63–77.
24. Liu, N.S., Loo, L.S., Loh, E., Seet, L.F., and Hong, W. (2009). Participation of Tom1L1 in EGF-stimulated endocytosis of EGF receptor. EMBO J. *28*, 3485–3499.
25. Abas, L., Benjamins, R., Malenica, N., Paciorek, T., Wiśniewska, J., Moulinier-Anzola, J.C., Sieberer, T., Friml, J., and Luschnig, C. (2006). Intracellular trafficking and proteolysis of the Arabidopsis auxin-efflux facilitator PIN2 are involved in root gravitropism. Nat. Cell Biol. *8*, 249–256.

26. Kleine-Vehn, J., Leitner, J., Zwiewka, M., Sauer, M., Abas, L., Luschnig, C., and Friml, J. (2008). Differential degradation of PIN2 auxin efflux carrier by retromer-dependent vacuolar targeting. Proc. Natl. Acad. Sci. USA *105*, 17812–17817.
27. Band, L.R., Wells, D.M., Larrieu, A., Sun, J., Middleton, A.M., French, A.P., Brunoud, G., Sato, E.M., Wilson, M.H., Péret, B., et al. (2012). Root gravitropism is regulated by a transient lateral auxin gradient controlled by a tipping-point mechanism. Proc. Natl. Acad. Sci. USA *109*, 4668–4673.
28. Reyes, F.C., Buono, R., and Otegui, M.S. (2011). Plant endosomal trafficking pathways. Curr. Opin. Plant Biol. *14*, 666–673.